European Journal of Medicinal Chemistry 46 (2011) 825–834

Contents lists available at ScienceDirect

European Journal of Medicinal Chemistry

journal homepage: http://www.elsevier.com/locate/ejmech

Original article

# Synthesis, molecular docking and binding studies of selective serotonin transporter inhibitors

Susanna Nencetti [a,*], Maria R. Mazzoni [b], Gabriella Ortore [a], Annalina Lapucci [a], Janette Giuntini [b], Elisabetta Orlandini [a], Irene Banti [a], Elisa Nuti [a], Antonio Lucacchini [b], Gino Giannaccini [b], Armando Rossello [a]

[a] Dipartimento di Scienze Farmaceutiche, Università di Pisa, Via Bonanno 6, 56126 Pisa, Italy
[b] Dipartimento di Psichiatria, Neurobiologia, Farmacologia e Biotecnologie, Facoltà di Farmacia, Università di Pisa, Via Bonanno 6, 56126 Pisa, Italy

ARTICLE INFO

*Article history:*
Received 2 July 2010
Received in revised form
14 December 2010
Accepted 14 December 2010
Available online 22 December 2010

*Keywords:*
Serotonin transporter inhibitors
Neurotransmitters
Piperidine oxime ether derivatives
Molecular docking

ABSTRACT

With the aim of obtaining compounds possessing high SERT selectivity, in the present work we synthesized and studied the inhibition of serotonin (SERT), dopamine (DAT) and norepinephrine (NET) transporters by docking studies and experimental binding measurements of a series of 4-(aryl)piperidin-3-one *O*-4-benzyl oxime hydrochlorides (**1**–**10**) of both *E* and *Z* configuration. *E* configuration compounds showed high SERT binding affinities ($K_i = 10–98$ nM) and high SERT selectivities over both NET and DAT. The molecular docking studies allowed a rationalization of the molecular basis of drug-SERT interactions both of the synthesized compounds and paroxetine and fluoxetine used as reference antidepressant drugs.



## 1. Introduction

Monoamine transporters i.e. the serotonin transporter (SERT), norepinephrine transporter (NET) and dopamine transporter (DAT) play an important role in maintaining the concentration of biogenic amine in the central nervous system (CNS) by transporting monoamines across neuronal membranes into presynaptic nerve cells. SERT is part of the large family of $Na^+/Cl^-$ dependent membrane transporters [1–4] and is a 630-aminoacid protein and believed to have 12 transmembrane domains.

SERT has great clinical importance as a molecular target for selective serotonin re-uptake inhibitors (SSRIs) such as fluoxetine, paroxetine and citalopram (Fig. 1) which exert their antidepressant action by preventing the binding of serotonin to its recognition site on the SERT and therefore by enhancing the concentration of this neurotransmitter in the synaptic cleft. Due to their favourable side effects profile and safety over a wide-dose range when compared with traditional tricyclic antidepressants (TCAs), they have dominated the market of antidepressants becoming the most widely prescribed pharmacological treatment for depression [5–9]. The breadth of their therapeutic profile has allowed their use for treating panic disorders (PD), post traumatic stress disorders (PTSD), social phobia, pre-menstrual dysphoric disorder (PMDD), obsessive–compulsive disorders (OCD) and anorexia [10,11].

Despite the fact that SSRIs generally possess good tolerability and have a reasonable safety profile, 2–4 weeks delay for the onset of action and side effects such as anxiety, sleep disturbance, sexual dysfunction and gastrointestinal intolerance remain as considerable barriers to effective therapy [12–14]. During the last decade fluoxetine, paroxetine and other SSRIs have been found to possess secondary binding properties among which dopamine (DA) and/or norepinephrine (NE) re-uptake inhibition, so that they are not so selective as initially thought [15–17]. In fact, only escitalopram, the active enantiomer (S(+)) of citalopram used for the treatment of depression and anxiety disorders, has been reconfirmed as a pure SSRI [18–21]. Knowledge of the additional properties of SSRIs sometimes helps the physician in selecting the SSRIs suitable to the clinical profile of the patient and allows their use in other clinical settings outside psychiatry. On the contrary, when the secondary binding properties are considered as undesirable side effects, the use of drugs with greater selectivity for SERT and without appreciable secondary binding properties may be recommended [22]. In this

* Corresponding author. Tel.: +39 050 2219559; fax: +39 050 2219605.
*E-mail address:* nencettis@farm.unipi.it (S. Nencetti).

0223-5234/$ – see front matter © 2010 Elsevier Masson SAS. All rights reserved.
doi:10.1016/j.ejmech.2010.12.018

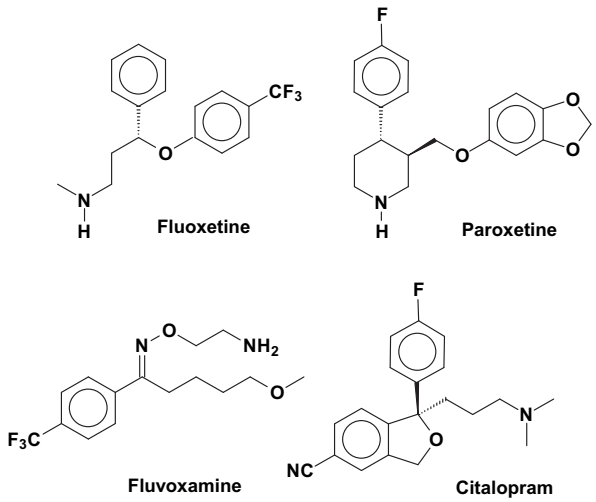


**Fig. 1.** Representative structure of some widely used SSRIs.

context the search for highly SERT selective SSRIs still remains an important goal offering significant advantages with regards to tolerability.

Heterocyclic compounds carrying piperidine skeleton are attractive targets of organic synthesis, moreover piperidine-based compounds with substituents at carbons 3 and 4 have been documented as potent antidepressant agents [23]. With the aim of obtaining new SSRIs with enhanced selectivity towards SERT, in the present work we designed and studied a series of piperidine oxime ether derivatives of general structure **A** (Fig. 2).

These new heterocyclic compounds (**A**) present an arylmethylenoxyimino moiety ($ArCH_2ON$=) in the 3 position and an aryl substituted moiety in the 4 position of the piperidine ring. The choice to introduce an oximethereal moiety, as found in fluvoxamine structure (Fig. 1), as part of the linker between the aminic portion and the β ring was due to the observation that the replacement of an $ArOCH_2$ group, as found in some SERT inhibitors, with an arylmethylenoxyimino ($ArCH_2ON$=C) or aryliminoxymethyl (ArCH=$NOCH_2$) moiety leads to compounds with improved biological activity compared to the parent compounds [24–26].

The R and $R_1$ substituents (F, $CF_3$, Cl) on the α and β aromatic moieties of compounds **A** are the most frequently present in antidepressant agents clinically used. Moreover to understand the molecular basis of compounds **1**–**10** interactions with monoamine transporters we performed a docking study using the structural information about SERT, DAT, NET provided by the models of the transporters constructed by Ravna et al. [4].

This paper reports the synthesis, the docking studies and the binding properties of 4-(aryl)piperidin-3-one *O*-4-benzyl oxime derivatives of both *E* and *Z* configuration (**1**–**10**, see Table 1) towards SERT, NET and DAT.

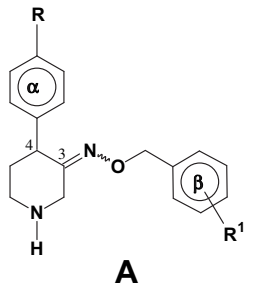


**Fig. 2.** General structure of the new piperidine oxime ether derivatives **A**.

## 2. Chemistry

The general methods for synthesis of *E* and *Z* 4-(aryl)piperidin-3-one *O*-4-benzyl oxime **1**,**3**,**5**,**7**,**9** and **2**,**4**,**6**,**8**,**10**, respectively, are shown in Scheme 1. 1-Benzyl-4-piperidone (**11**) was reacted with the appropriate aryl Grignard reagent in tetrahydrofuran (THF) at reflux temperature to give the 4-piperidinols **12** and **13** in good yields. Then, the 4-hydroxyl group was removed by dehydratation with *p*-toluensulfonic acid (PTSA) in benzene to give the 3,4-dehydro piperidines **14** and **15**. Hydroboration with borane-methyl sulfide complex of the olefinic double bond of **14** and **15** followed by treatment with hydrogen peroxide and sodium hydroxide gave the diastereomeric mixture of 3-piperidinols **16** and **17** which, without separation, were oxidized under Swern conditions to the corresponding keto compounds **18** and **19**. The reaction of **18** and **19** with hydroxylamine hydrochloride gave the *E*/*Z* mixture of the oximes **20** and **21** which were alkylated with the appropriate benzyl chlorides to yield the *Z* oxime ether isomers **22**–**26**, exclusively. Catalytic hydrogenolysis of **22**–**26** in acidic medium gave the *E*/*Z* mixture (1:1.5) of the 4-(aryl)piperidin-3-one *O*-4-benzyl oxime hydrochlorides (**1**–**10**) from which the compounds of *E* (**1**,**3**,**5**,**7**,**9**) and *Z* (**2**,**4**,**6**,**8**,**10**) configuration were then isolated by preparative TLC.

The configuration around the N=C double bond of the couples of the oxime ether derivatives was assigned on the basis of a comparison of their $^1$H NMR spectral data. In the compounds of *E* configuration (**1**,**3**,**5**,**7**,**9**) the proton linked to the C(4) of the piperidine ring ($H_4$) resonates at lower fields with respect to the same hydrogen in the compounds of *Z* configuration (**2**,**4**,**6**,**8**,**10**) (1.10–1.13 ppm). This fact may be attributed to the paramagnetic effect of the spatially proximal oximethereal oxygen. On the contrary in the compounds of *Z* configuration it is the protons linked to the C(2) of the piperidine ring ($H_2$ and $H_2'$) which, being on the same side as the oximethereal oxygen, that resonate at lower fields with respect to the same hydrogen of the corresponding *E* isomers [27] (0.16–0.25 and 0.40–0.45 ppm).

## 3. Pharmacological evaluation

All the synthesized compounds of both *E* (**1**,**3**,**5**,**7**,**9**) and *Z* (**2**,**4**,**6**,**8**,**10**) configuration were evaluated as a racemic mixture for their ability to interfere with the system of 5-HT, NE and DA transmission by evaluating their ability to inhibit the binding of specific radioligands to SERT and NET in rabbit cortical membranes and to DAT in rabbit striatal membranes. [$^3$H]-Paroxetine and [$^3$H]-nisoxetine were used as specific radiolabelled ligand for SERT and NET, respectively while [$^3$H]WIN 35,428 was used to label DAT. The structure, the $K_i$ values, calculated using the Cheng-Prusoff equation [28], and selectivity ratio for compounds **1**–**10** are shown in Table 1 together with those obtained in the same assays for fluoxetine and paroxetine used as reference drugs.

The results of binding assays reported in Table 1 show that all the synthesized compounds (**1**–**10**) were able to inhibit [$^3$H]-paroxetine binding to SERT with $K_i$ values in the nanomolar range. The most active compounds of this series were the oxime ether derivatives of *E* configuration **1**, **5** and **9** and the *Z* compound **6** with $K_i$ values ranging from 10.28 (compound **9**) to 81.07 nM (compound **6**). *E* configuration compounds **3** and **7** and the *Z* compound **10** were slightly less active ($K_i$ values: 98.42, 96.82, and 96.58 nM, respectively) while the *Z* compounds **2**, **4** and **8** were those with the highest $K_i$ values ($K_i > 100$ nM). In the same kind of assay, fluoxetine and paroxetine showed $K_i$ values of 5.80 and 0.31 nM, respectively.

A comparison between the $K_i$ values of *E* and *Z* isomers showed differences between the diastereomeric couples. Compound **3** was 1.4-fold more potent than **4**, compound **5** was 3.6 fold more potent than **6**, compound **7** was 4-fold more potent than **8**, compounds **1**

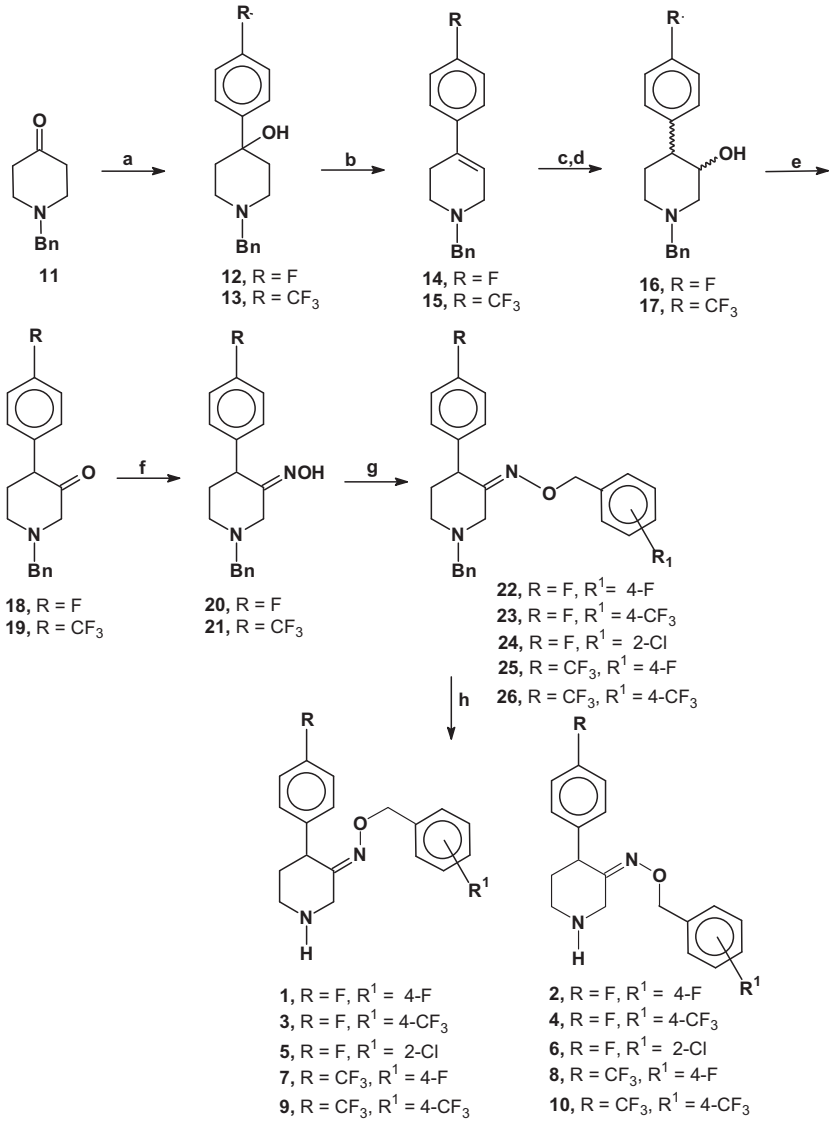


**Scheme 1.** a: ArMgBr, an.THF, reflux; b: PTSA, $C_6H_6$, reflux; c: $BH_3(CH_3)_2S$, an.THF; d: $H_2O_2$, NaOH ; e: $(COCl)_2$,DMSO, $Et_3N$, $CH_2Cl_2$; f: $NH_2OH$ HCl/$H_2O$, $CH_2Cl_2$; g: NaH, an.THF, appropriate Ar-$CH_2X$, DMF; h: $H_2$, Pd/C, EtOH, EtOH·HCl.

and **9** were about 10-fold more potent than **2** and **10**, respectively. In Fig. 3 are shown the displacement curves of [$^3$H]paroxetine binding to cortical membranes by diastereoisomeric couple of compounds **9** (*E*), **10** (*Z*).

In the case of *Z* configuration derivatives, the data reported in Table 1 showed that only **6** and **10** possess $K_i$ values lower than 100 nM while compounds **2**, **4**, **8** exhibited $K_i$ values higher than 100 nM. Moreover, an analysis of the biological data shown in Table 1 revealed that in type **A** compounds, the chlorine atom in the 2 position on the benzylic group (β ring, Fig. 2) was the substituent that confers the best affinity for SERT independently of the substituent (fluorine atom or a trifluoromethyl group) on the aromatic ring directly linked to the piperidine nucleus (α ring, Fig. 2).

As regards the ability of synthesized compounds (**1**–**10**) to inhibit [$^3$H]WIN 35,428 binding to DAT, *Z* configuration compounds **2**,**4**,**6**,**8**,**10** showed $K_i$ values in the micromolar range while those of *E* configuration **1**,**3**,**5**,**7**,**9** were practically inactive (Table 1).

Comparison of the $K_i$ values of all the compounds for SERT and DAT showed that *E* configuration compounds possessed high selectivity for SERT with DAT/SERT ratio ranging from ≅300 for **1** to >9000 for **3**, **7**, **9**. Such selectivity was reduced for *Z* configuration compounds (DAT/SERT ratio ranging from 7 for compound **8** to 118 for compound **6**) since they were better inhibitors of [$^3$H]WIN 35,428 binding to DAT.

In order to better define the selectivity profile of the most active *E* configuration compounds (compounds **1**,**3**,**7** and **9**), their ability to inhibit $^3$[H]-nisoxetine binding to NET in rat cortical membranes was also evaluated. The data reported in Table 1 indicate that these compounds were very weak inhibitors of $^3$[H]-nisoxetine binding to NET with $K_i$ values ranging from 9300 for compound **7** to 19,500 μM for compound **3**. A comparison of $K_i$ values of all the compounds for SERT and NET showed that *E* configuration compounds possessed high selectivity for SERT with the NET/SERT ratio ranging from ≅96 for **7** to 972 for **9**.

Most of the compounds meet the "druglike" criteria [29] having MW < 500 and ClogP values (see the Supporting Information) in the range deemed suitable for penetration of the blood-brain barrier.

## 4. Molecular docking

In order to rationalize activity trends, molecular docking of paroxetine, fluoxetine and compounds **1**–**10** was performed in the

**Table 1**
Inhibition constant values ($K_i$)[a] of oxime ethers **1**–**10**, fluoxetine and paroxetine for inhibition of [$^3$H]paroxetine, [$^3$H]-nisoxetine and [$^3$H]WIN 35,428 binding to SERT, NET and DAT.

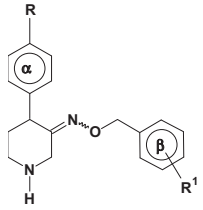


| Compd[b] | R | R$^1$ | | SERT[c] | DAT[d] | NET[e] | NET/SERT[f] | DAT/SERT[f] |
|---|---|---|---|---|---|---|---|---|
| | | | | $K_i$ (nM) | $K_i$ (nM) | $K_i$ (nM) | | |
| **1** | F | 4-F | *E* | 28.74 ± 7.03 | 9460 ± 2160 | 13,400 ± 1570 | 466 | 329 |
| **2** | F | 4-F | *Z* | 305.90 ± 71.01 | 3190 ± 70 | nt[g] | | 10 |
| **3** | F | 4-$CF_3$ | *E* | 98.42 ± 17.14 | >100,000 | 19,500 ± 2100 | 198 | >1000 |
| **4** | F | 4-$CF_3$ | *Z* | 138.61 ± 20.79 | 6200 ± 270 | nt[g] | | 45 |
| **5** | F | 2-Cl | *E* | 22.60 ± 3.53 | 12,900 ± 1040 | 11,200 ± 1300 | 496 | 571 |
| **6** | F | 2-Cl | *Z* | 81.07 ± 5.30 | 3800 ± 600 | nt[g] | | 47 |
| **7** | $CF_3$ | 4-F | *E* | 96.82 ± 1 4.80 | >100,000 | 9300 ± 1000 | 96 | >1000 |
| **8** | $CF_3$ | 4-F | *Z* | 396.50 ± 17.60 | 2800 ± 300 | nt[g] | | 7 |
| **9** | $CF_3$ | 2-Cl | *E* | 10.28 ± 3.89 | >100,000 | 10,000 ± 1200 | 972 | >9000 |
| **10** | $CF_3$ | 2-Cl | *Z* | 96.58 ± 14.80 | 4200 ± 700 | nt[g] | | 43 |
| | **Fluoxetine** | | | 5.80 ± 2.90 | 4000 ± 1700 | 609.00 ± 50.00 | 105 | 670 |
| | **Paroxetine** | | | 0.31 ± 0.018 | 769[h] | 80.00 ± 10.00 | 258 | 2480 |
| | **GBR12909** | | | | 1.5 ± 0.2 | | | |
| | **Nisoxetine** | | | | | 3.5 ± 0.8 | | |

[a] Compounds tested at concentrations from 1 nM to 10 mM. Values represent the mean ± s.e.m. of 3 separate experiments.
[b] Prepared and tested as hydrochloride salts.
[c] Values determined using [$^3$H]-paroxetine as radioligand.
[d] Values determined using [$^3$H]-WIN 35,428 as radioligand.
[e] Values determined using [$^3$H]-nisoxetine as radioligand.
[f] Ratios of $K_i$ values.
[g] Not tested.
[h] $K_i$ value represents average of at least two independent experiments.

homology models of SERT, DAT and NET constructed by Ravna et al. [4], using LeuT as a template [1]. Compounds were docked in the central binding pocket 1 of SERT, DAT and NET, corresponding to the substrate binding pocket of leucine in the $LeuT_{Aa}$ crystal structure, using the GOLD program. The principal ligand–receptor interactions were analysed, and the best orientation of the newly synthesized compounds was compared to the paroxetine one. In accordance with previously reported docking studies on SERT ligands [30–32], paroxetine occupies a cavity delimited by TM1, TM3, TM6 and TM8,

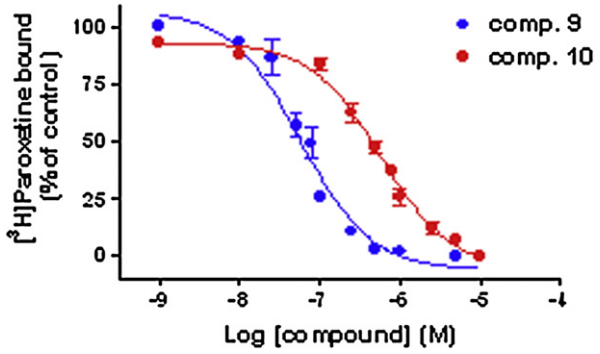


**Fig. 3.** Displacement of [$^3$H]paroxetine binding to cortical membranes by compounds and **9** (*E*), **10** (*Z*). Membranes were incubated in duplicate with [$^3$H]paroxetine in the presence and absence of increasing concentrations of each compound as described in Experimental section. Data points represent the means ± s.e.m. of three independent experiments.

and in particular engages an ionic interaction between the protonated N of piperidine and Asp98 (Fig. 4a–c). The piperonilic moiety interacts with Asn177 and with the non-conserved Thr439, in analogy with the proposed binding mode of 5-HT [2], that allows the same ionic interaction with Asp98 and a hydrogen bond between the hydroxyl group of 5-HT and Thr439. The fluorophenyl moiety of paroxetine is stabilized through a stacking with Phe341 and inserted in a pocket defined by Tyr95, Ala169, Ile172, Val343, apart from Phe341. Also fluoxetine has a similar binding mode, but the $CF_3$ cannot interact with the same strength of the piperonilic moiety of paroxetine with Asn177 and Thr439 (Fig. 4c).

As shown in Fig. 4a, the new compounds of *E* configuration seem to be able to overlap the orientation of paroxetine in the binding site, with three points of interaction: the piperidine nitrogen with Asp98, the R substituent (see Table 1) with Tyr95, and the $R_1$ group (see Table 1) with Asn177 and Thr439. This binding mode is independent of their chirality, with the only exception of compound **3** (yellow in Fig. 4a), whose fluorosubstituted α ring of the *R* enantiomer directs away from the paroxetine one.

The presence of a bulkier substituent like $CF_3$ in *para* position, when also the second phenyl bears a substituent in *para* position, makes the contact unfavourable with the binding site surface. As shown in Fig. 4d, the $CF_3$ of compounds **3** and **7**, nevertheless the effective orientation in SERT of these compounds, creates a steric clash with the atoms of the cavity walls, whose surface represented in Fig. 4d is forced by the threefluoromethyl group. This could explain the higher affinity of compounds **1**, **5** and **9** for SERT, with respect to compounds **3** and **7**. Compounds of *Z* configuration (Fig. 4b) do not overlap the paroxetine orientation, because their oximic chains lie

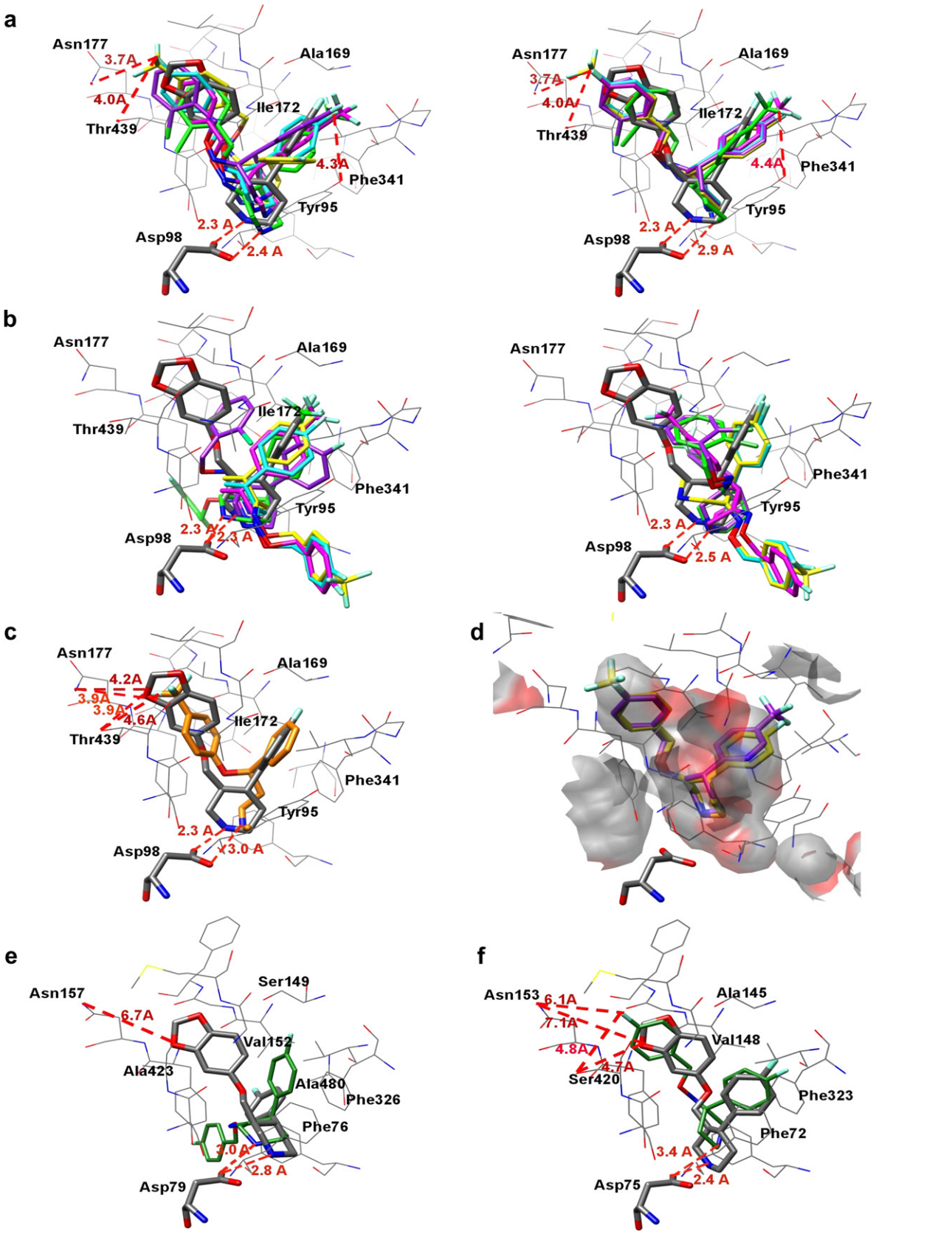


**Fig. 4.** Docking orientations of compounds: a) (*R*)-1 (cyan), (*R*)-3 (yellow), (*R*)-5 (purple), (*R*)-7 (magenta), (*R*)-9 (green) and (3*S*,4*R*)-paroxetine (grey) into SERT on the left; (*S*)-1 (cyan), (*S*)-3 (yellow), (*S*)-5 (purple), (*S*)-7 (magenta), (*S*)-9 (green) and (3*S*,4*R*)-paroxetine (grey) into SERT on the right; b) (*R*)-2 (cyan), (*R*)-4 (yellow), (*R*)-6 (purple), (*R*)-8 (magenta), (*R*)-10 (green) and (3S,4R)-paroxetine (grey) into SERT on the left; (*S*)-2 (cyan), (*S*)-4 (yellow), (*S*)-6 (purple), (*S*)-8 (magenta), (*S*)-10 (green) and (3*S*,4*R*)-paroxetine (grey) into SERT on the right; c) (*R*)-fluoxetine (orange) compared to (3S,4R)-paroxetine (grey) into SERT; d) (*S*)-3 (yellow) and (*S*)-5 (purple) in the SERT binding site, whose Van der Waals surface is represented in grey; e) 1 (green), as a model compound compared to (3*S*,4*R*)-paroxetine (grey) into DAT; f) 1 (green), as a model compound compared to (3*S*,4*R*)-paroxetine (grey) into NET. (For interpretation of the references to colour in this figure legend, the reader is referred to the web version of this article).

generally out of the binding site. The docking of compounds **2**, **4** and **8** is very similar, and independent of their enantiomeric configuration. The *ortho*-substituted compounds **6** and **10** have a different orientation compared to the other *Z* derivatives: in both the *R* and *S* configuration compounds **6** assumes in SERT a collapsed orientation which allows a partial superposition on the paroxetine. This compound showed an affinity of 81.07 nM, the best value among the compounds of *Z* configuration.

Thus, analyzing the docking results, the *E* configuration of our oxime ethers and the absence of bulky substituents in *para* position of the phenyls seem to be determinant for the affinity towards SERT. On the contrary, the enantiomeric configuration of compounds **1**–**10** seems to have no significant effects on the interaction of these compounds with the SERT binding site.

As regards the docking into DAT (Fig. 4e), all compounds assume a different orientation in this transporter. Paroxetine interacts with Asp79 (corresponding to Asp98 in SERT), and its piperonilic ring occupies the same cavity as in SERT, but the presence of Phe76 and Ala423 in place of Tyr95 and Thr439 causes a slight shift of the ligand towards Phe326 in DAT, thus causing the lack of the hydrogen bond with the hydroxyl group of the Thr439. Furthermore, the fluorophenyl ring prefers another collocation instead of the interaction with Ser149, which replaces Ala169 of the SERT and makes the region less accessible. The fluorophenyl ring lies in a cavity peculiar to DAT, due to the presence of the non-conserved residues Val152 and Ala480 which open a larger space compared to Ile172 and Thr497 of SERT, but cannot allow any effective interaction with the binding site (Fig. 4e). Fig. 4e also represents the general arrangement of compounds **1**–**10** in DAT (compound **1** is reported in figure as an example), which is different from the paroxetine one. The model compound **1** occupies the same cavities of the transporter without important interactions with residues except for the ionic bond with Asp79. This kind of binding mode is in agreement with the affinity trend of all the synthesized compounds, characterized by a very low affinity for DAT.

The third transporter, NET, presents a very high homology with DAT in the binding site (>80%), and all the residues previously reported as representative residues for the interaction of DAT with the ligands are conserved, except for the one corresponding to Ala423 of DAT and Thr439 of SERT, which in NET is Ser420. The presence of this serine allows a docking of the ligands similar to the SERT one (Fig. 4f): the piperonilic moiety of paroxetine engages a weak interaction with the non-conserved Ser420 but loses the interaction with Asn153 (Asn177 in SERT) because it shifts about 2.5 Å with respect to its position in the SERT. This different arrangement is due to the preferred insertion of the paroxetine fluorophenyl ring between Phe72, lacking in SERT, and Phe323. The *E* configuration compounds **1**, **3**, **5**, **7** and **9** are oriented in a similar manner (Fig. 4f, compound **1** is reported as a model compound), but could engage only weak polar interactions between the substituent on the phenyl β ring and Ser420, and between the protonated amine and Asp79. The presence of Phe72 instead of Tyr95 hampers further interactions of the substituent on the phenyl α ring, that are peculiar to the SERT binding mode.

The docking performed in SERT, DAT and NET highlights the role of the SERT Thr439 substitution with DAT Ala423 and NET Ser420 in directing the orientation of the ligands in the binding site and the importance of the Tyr95/Phe76/Phe72, Ala169/Ser149/Ala145, Ile172/Val152/Val148, Thr497/Ala480/Ala477 replacements in SERT/DAT/NET in determining a different stabilization of compounds in the three transporters. Furthermore, the contribution of Asn177 and/or Thr439 in the polar interaction with the ligands seems to be determinant for an effective binding in SERT. The lack or the lessening of these interactions in DAT and NET precludes any significant activity of the ligands.

## 5. Conclusion

In the present study we synthesized a series of *E* and *Z* 4-(aryl) piperidin-3-one *O*-4-benzyl oxime derivatives (**1**–**10**) in order to obtain new selective SERT inhibitors. The inhibition studies of [$^3$H] paroxetine, $^3$[H]-nisoxetine and [$^3$H]WIN 35,428 binding to SERT, NET and DAT showed that all the compounds, and particularly *E* configuration compounds (**1**,**3**,**5**,**7**,**9**), showed high SERT binding affinities ($K_i = 10–98$ nM) and high SERT selectivities since they are scarcely or practically inactive towards NET and DAT. These results are in accordance with the fact that only *E* configuration compounds can assume in the SERT binding site a favourable orientation in analogy with the proposed binding mode of 5-HT [2], which is also the same for paroxetine, while in DAT and NET the disposition of the compounds could not allow effective interactions.

The different substituents introduced on the α and β aromatic moieties played an important role in influencing the potency of compounds as SERT inhibitors. In particular the docking studies suggested that the concurrent *para*-substitution of both α and β aromatic moieties with almost one bulkier substituent, makes unfavourable the contact with the binding site surface determining a detrimental effect on the affinity. Moreover the enantiomeric configuration of compounds **1**–**10** seems to have no significant effects on the interaction of these compounds with the SERT binding site.

The most interesting compound in this series is **9** possessing an affinity for SERT in the same range as fluoxetine and an excellent SERT selectivity, higher than that of fluoxetine and paroxetine as well as a ClogP value (see the Supporting Information) in the range deemed suitable for penetration of the blood-brain barrier. Furthermore, **9** represents an attractive potential lead to further optimization by introducing small para substituents on β ring able to engage hydrogen bonds with Asn177 together with small ortho substituents to better define the SAR of this class of compounds.

## 6. Experimental section

### 6.1. Chemistry

Melting points were determined on a Köfler hot-stage apparatus and are uncorrected. IR spectra for comparison between compounds were recorded with a Perkin–Elmer mod.1310, as Nujol mulls in the case of solid substances, or as liquid film in the case of liquids. $^1$H NMR spectra were obtained with a Varian Gemini-200 MHz spectrometer in a ca. 2% solution of $CDCl_3$. Chemical shifts ($\delta$) are reported in parts per million (ppm) downfield from tetramethylsilane (TMS) and adjusted according to residual solvent peaks. Electron impact (EI, 70 eV) mass spectra were obtained on a HP-5988A mass spectrometer. Reactions were monitored by TLC on silica gel plates (Merck Silica Gel 60 $F_{254}$), spots were detected under UV light. Preparative TLC were performed with silica gel plates (2 mm, Merck Silica Gel 60 $F_{254}$). Chromatographic separations were performed using Merck silica gel (70–230 mesh). $Na_2SO_4$ was always used as the drying agent. Evaporation was carried out "in vacuo" (rotating evaporator). Elemental analyses were performed by our analytical laboratory and agreed with theoretical values to within ±0.4%.

#### 6.1.1. 1-Benzyl-4-(4-fluorophenyl)-(*12*) and 1-benzyl-4-(4-(trifluoromethyl)phenyl)-(*13*) piperidin-4-ol

The opportune 4-(aryl)-magnesium bromide was prepared in the usual manner from 4-fluoro or 4-trifluoromethyl bromobenzene (0.015 mol), magnesium turning (0.015 g-atom) and anhydrous THF (20 mL). The reaction mixture was then diluted with anhydrous THF (30 mL), refluxed under stirring for 30 min and

treated dropwise at room temperature with a solution of N-benzyl-4-piperidone (**11**) (1.4 g, 0.0075 mol) and anhydrous THF (18 mL). After total addition, the solution was refluxed under stirring for 15 h, then quenched after cooling by the addition of iced water (10 mL) and extracted three times with EtOAc. The combined organic phases were dried and evaporated to yield an oily residue that was crystallized from hexane to give pure **12** as a pale yellow solid, or purified by column chromatography on silica gel (EtOAc/hexane 4:6) to give pure **13** as a white solid. **12**: (73%) mp: 78–80 °C; $^1$H NMR [33] (200 MHz, $CDCl_3$): $\delta = 7.49$ (m, 2H), 7.32 (m, 5H), 7.04 (m, 2H), 3.61 (s, 2H), 2.82 (m, 2H), 2.50 (m, 2H), 2.16 (m, 2H), 1.74 ppm (m, 3H); MS (EI, 70 eV) *m/z* (%): 285 (7); 91 (100) $[M + H]^+$; Anal. calcd for $C_{18}H_{20}FNO$: C 75.76, H 7.06, N 4.91, found: C 75.49, H 7.28, N 4.73. **13**: (85%) mp: 127 °C; $^1$H NMR (200 MHz, $CDCl_3$): $\delta = 7.63$ (m, 4H), 7.32 (m, 5H), 3.64 (s, 2H), 2.86 (m, 2H), 2.52 (m, 2H), 2.22 (m, 2H), 1.73 ppm (m, 3H); MS (EI, 70 eV) *m/z* (%): 335 (9); 91 (100) $[M + H]^+$; Anal. calcd for $C_{19}H_{20}F_3NO$: C 68.05, H 6.01, N 4.18, found: C 68.38, H 6.19, N 4.07.

### 6.1.2. 1-Benzyl-4-(4-fluorophenyl)-(**14**) and 1-benzyl-4-(4-(trifluoromethyl)phenyl)-(**15**) 1,2,3,6-tetrahydropyridine

The appropriate alcohol **12**, **13** (7.3 mmol) was dissolved in anhydrous benzene (50 mL) containing PTSA (11 mmol, 2.1 g). The mixture was heated to reflux with azeotropic removal of water until no further water was collected. After cooling at room temperature the solution was washed with saturated aqueous $NaHCO_3$, dried and evaporated to yield pure **14** and **15** as yellow solids. **14**: (96%) mp: 48–50 °C; $^1$H NMR [34] (200 MHz, $CDCl_3$): $\delta = 7.31$ (m, 7H), 6.99 (t, $J = 8.8$ Hz, 2H), 5.98 (m, 1H), 3.62 (s, 2H), 3.14 (m, 2H), 2.72 (t, $J = 5.8$ Hz, 2H), 2.53 ppm (m, 2H). IR (KBr): $\nu = 1620$ cm$^{-1}$; MS (EI, 70 eV) *m/z* (%): 267 (48); 91 (100) $[M + H]^+$; Anal. calcd for $C_{18}H_{19}FN$: C 80.87, H 6.79, N 5.24, found: C 80.63, H 6.91, H 5.12. **15**: (72%) mp: 87 °C; $^1$H NMR (200 MHz, $CDCl_3$): $\delta = 7.55$ (m, 4H), 7.39 (m,5H), 6.11 (m, 1H), 3.60 (s, 2H), 3.13 (m, 2H), 2.71 (t, $J = 5.8$ Hz, 2H) 2.48 ppm (m, 2H); IR (KBr): $\nu = 1620$ cm$^{-1}$; MS (EI, 70 eV) *m/z* (%): 317 (48); 91 (100). Anal. calcd for $C_{19}H_{18}F_3NO$: C 71.91, H 5.72, N 4.41, found: C 71.73, H 5.57, N 4.26.

### 6.1.3. 1-Benzyl-4-(4-fluorophenyl) (**16**) and 1-benzyl-4-(4-(trifluoromethyl)phenyl) (**17**) piperidin-3-ol

A 2 M solution of $BH_3 \cdot (CH_3)_2S$ complex in anhydrous THF (14.6 mmol, 7.4 mL) was added dropwise to a cooled (0 °C) stirred solution of **14** or **15** (4.8 mmol) in anhydrous THF (22 mL). The mixture was then stirred at room temperature for 3 days. Water (0.3 mL) was then carefully added, heated at 40 °C, then NaOH 10% (1.2 mL) and $H_2O_2$ 36% (1 mL) added and stirred for 1 h. The reaction mixture was then extracted with $Et_2O$ and combined organic layers washed with water and evaporated to yield an oil that was chromatographed on silica gel column (EtOAc/hexane 4:6) to give **16**, **17** as solids. **16**: (66%) mp: 89–91 °C; $^1$H NMR (200 MHz, $CDCl_3$): $\delta = 7.29$ (m, 7H), 7.11 (m, 2H), 3.79 (dt, $J = 9.8$, 4.4 Hz, 1H), 3.63, 3.65 (2d, $J = 13.2$ Hz, 2H), 3.18 (dd, $J = 10.5$, 4.4 Hz, 1H), 2.93 (d, $J = 11.2$ Hz, 1H), 2.39 (m, 1H), 1.99 (m, 2H), 1.80 ppm (m, 2H); IR (KBr): $\nu = 3468$ cm$^{-1}$; MS (EI, 70 eV) *m/z* (%): 285 (9); 91 (100); Anal. calcd for $C_{18}H_{20}FNO$: C 75.76, H 7.06, N 4.91, found: C 75.92, H 6.93, N 4.82. **17**: (42%) mp: 105 °C; $^1$H NMR (200 MHz, $CDCl_3$): $\delta = 7.61$ (m, 2H), 7.35 (m, 7H), 3.90 (m, 1H), 3.66, 3.58 (2d, $J = 13$ Hz, 2H), 3.21 (dd, $J = 10.6$, 4.5 Hz, 1H), 2.97 (d, $J = 11$ Hz, 1H), 2.51 (m, 1H), 1.99 (m, 2H), 1.86 ppm (m, 2H); IR (KBr): $\nu = 3465$ cm$^{-1}$; MS (EI, 70 eV) *m/z* (%): 335 (10); 91 (100); Anal. calcd for $C_{19}H_{20}F_3NO$: C 68.05, H 6.01, N 4.18,. found: C 68.31, H 6.23, N 4.36.

### 6.1.4. 1-Benzyl-4-(4-fluorophenyl) (**18**) and 1-benzyl-4-(4-(trifluoromethyl)phenyl) (**19**) piperidin-3-one hydrochlorides

A solution of oxalyl chloride (2.9 mmol, 0.25 mL) in $CH_2Cl_2$ (13 mL) was cooled to −78 °C with stirring under a nitrogen atmosphere. A solution of DMSO (5.8 mmol, 0.4 mL) in $CH_2Cl_2$ (20 mL) was added dropwise. The reaction mixture was then stirred for 15 min. A solution of the appropriate alcohol **16** or **17** (2.2 mmol) in $CH_2Cl_2$ (20 mL) was added dropwise and then the reaction mixture was stirred at −60 °C for 15 min. The reaction mixture was cooled to −78 °C and $Et_3N$ (8.7 mmol, 1.21 mL) was added in one portion. The reaction mixture was warmed to room temperature over 6 h, and then poured into water, mixed, and extracted three times with $Et_2O$. The organic extracts washed with water, dried and evaporated gave a crude oil that was purified by column chromatography on silica gel (EtOAc/hexane 4:6) to give **18** and **19** as solids. **18** and **19** were suddenly converted into hydrochloride salts by dissolving in $Et_2O$ and treating with $Et_2O \cdot HCl$ to yield pure **18**·HCl and **19**·HCl. **18**·HCl (65%) mp: 170–172 °C; $^1$H NMR (200 MHz, $CDCl_3$): $\delta = 7.27$ (m, 5H), 7.07 (m, 2H), 6.98 (m.2H), 3.62 (s, 2H), 3.52 (m, 1H), 3.27 (m,1H), 3.06–2.57 (m,3H), 2.19 ppm (m, 2H); IR (KBr): $\nu = 1725$ cm$^{-1}$; Anal. calcd for $C_{18}H_{19}ClFNO$: C 76.30, H 6.40, N 4.94, found: C 76.19, H 6.25, N 4.78. **19**·HCl (61%) mp: 173–175 °C; $^1$H NMR (200 MHz, $CDCl_3$): $\delta = 7.60$ (m, 9H), 3.62 (s, 2H), 3.50 (m,1H), 3.23 (m, 1H), 3.02–2.57 (m, 3H), 2.17 ppm (m, 2H); IR (KBr): $\nu = 1720$ cm$^{-1}$; Anal. calcd for $C_{19}H_{19}ClF_3NO$: C 68.46, H 5.44, N 4.20, found: C 68.63, H 5.29, N 4.37.

### 6.1.5. 1-Benzyl-4-(4-fluorophenyl) (**20**) and 1-benzyl-4-(4-(trifluoromethyl)phenyl) (**21**) piperidin-3-one oxime

To a stirred solution of **18**·HCl or **19**·HCl (1.2 mmol) in $CH_2Cl_2$ (7 mL), was added a solution of hydroxylamine hydrochloride (1.4 mmol, 0.096 g) and water (8.3 mL). The reaction mixture was stirred vigorously at room temperature for 24 h. After separation of the aqueous phase $NaHCO_3$ was added and then extracted with $CH_2Cl_2$. The combined organic layers were evaporated to give a solid that was crystallized from EtOH, to give **20** and **21** as white solids. **20** (61%) mp: 187–189 °C; $^1$H NMR (200 MHz, $CDCl_3$) $\delta = 7.26$ (m, 7H), 7.0 (m, 2H), 4.12 (d, $J = 14$ Hz, 1H), 3.71, 3.58 (2d, $J = 13.2$ Hz, 2H), 3.45 (m, 1H), 2.81 (d, $J = 14$ Hz, 1H), 2.40 (m, 2H), 2.22–1.98 ppm (m, 2H); MS (EI, 70 eV) *m/z* 298 (8%), 91 (100%); Anal. calcd for $C_{18}H_{19}FN_2O$: C 72.46, H 6.42, N 9.39, found: C 72.65, H 6.61, N 9.25. **21** (55%) mp 180–181 °C; $^1$H NMR $\delta$ 7.30–6.92 (m, 9H), 4.11 (d, $J = 14$ Hz, 1H), 3.60 (m, 2H), 3.47 (m, 1H), 2.72 (d, $J = 14$ Hz, 1H), 2.38–1.89 (m, 4H); MS (EI, 70 eV) *m/z* (%): 340 (9%), 91 (100%); Anal. calcd for $C_{19}H_{19}F_3N_2O$ C 65.51, H 5.50, N 8.04; found: C 65.34, H 5.32, N 8.27.

### 6.1.6. General procedure for preparation of N-benzyl oxime ethers **22–26**

To a stirred solution of the oxime **20** or **21** (0.73 mmol) in anhydrous THF (10 mL) was added NaH 60% (0.78 mmol) under nitrogen atmosphere. The mixture was stirred for 1 h at room temperature then evaporated. The oxime sodium salt of **20** or **21** was dissolved in anhydrous DMF (3.9 mL) and added dropwise under stirring with a solution of the opportune benzyl chloride (0.78 mmol) in anhydrous DMF (2.3 mL). The mixture was then stirred under nitrogen at 50 °C for 5 days then added with water and extracted with $CH_2Cl_2$. The organic extracts were evaporated to yield a crude oil which was purified by column chromatography on silica gel (EtOAc/hexane 3:7) to yield the *Z* ether isomer **22–26**, exclusively.

#### 6.1.6.1. (Z)-1-Benzyl-4-(4-fluorophenyl)piperidin-3-one O-4-fluorobenzyl oxime (**22**).

(80%) $^1$H NMR (200 MHz, $CDCl_3$) $\delta = 7.33$–6.96 (m, 13H), 4.91 (s, 2H), 3.76 (d, $J = 14$ Hz, 1H), 3.59 (m, 2H); 3.52 (m, 1H), 3.07 (d, $J = 14$ Hz, 1H), 2.78 (m, 1H), 2.46 (m, 1H), 2.12 ppm (m, 2H); Anal. calcd for $C_{25}H_{24}F_2N_2O$: C 76.30, H 6.40, N 4.94, found: C 76.51, H 6.63, N 4.72.

#### 6.1.6.2. (Z)-1-Benzyl-4-(4-(trifluoromethyl)phenyl)piperidin-3-one O-4-fluorobenzyl oxime (**23**).

(85%); $^1$H NMR (200 MHz, $CDCl_3$)

$\delta$ = 7.64–6.93 (m, 13H), 5.01 (s, 2H), 3.78 (d, $J$ = 13.7, 1H), 3.61 (m, 2H), 3.55 (m, 1H), 3.09 (d, $J$ = 13.7, 1H), 2.80 (m, 1H), 2.49 (m, 1H), 2.12 ppm (m, 2H); Anal. calcd for $C_{26}H_{24}F_4N_2O$: C 68.41, H 5.30, N 6.14, found: C 68.63, H 5.19, N 6.27.

*6.1.6.3. (Z)-1-Benzyl-4-(4-fluorophenyl)piperidin-3-one O-2-chlorobenzyl oxime (**24**).* (73%) $^1$H NMR (200 MHz, $CDCl_3$) $\delta$ = 7.23 (m, 11H), 6.98 (m, 2H), 5.10 (s, 2H); 3.80 (d, $J$ = 14 Hz, 1H), 3.62 (s, 2H), 3.58 (m, 1H), 3.19 (d, $J$ = 14 Hz, 1H,), 2.79 (m, 1H), 2.51 (m, 1H), 2.10 ppm (m, 2H); Anal. calcd for $C_{25}H_{24}FClN_2O$: C 71.00, H 5.72, N 6.62, found: C 71.19, H 5.59, N 6.77.

*6.1.6.4. (Z)-1-Benzyl-4-(4-(trifluoromethyl)phenyl)piperidin-3-one O-4-fluorobenzyl oxime (**25**).* (66%) $^1$H NMR (200 MHz, $CDCl_3$) $\delta$ = 7.58–6.99 (m, 13H), 4.91 (2s, 2H), 3.79 (d, $J$ = 14 Hz, 1H,), 3.64 (s, 2H), 3.55 (m, 1H), 3.17 (d, $J$ = 14 Hz, 1H), 2.80 (m, 1H), 2.52 (m, 1H), 2.10 ppm (m, 2H); Anal. calcd for $C_{26}H_{24}F_4N_2O$: C 68.41, H 5.30, N 6.14, found: 68.27, H 5.46, 6.29.

*6.1.6.5. (Z)-1-Benzyl-4-(4-(trifluoromethyl)phenyl)piperidin-3-one O-2-chlorobenzyl oxime (**26**).* (41%) $^1$H NMR (200 MHz, $CDCl_3$) $\delta$ = 7.50–6.95 (m, 13H), 4.93 (s, 2H), 3.80 (d, $J$ = 14 Hz, 1H), 3.64 (s, 2H), 3.57 (m, 1H), 3.13 (d, $J$ = 14 Hz, 1H), 2.80 (m, 1H), 2.52 (m, 1H), 2.11 ppm (m, 2H); Anal. calcd for $C_{26}H_{24}F_3ClN_2O$: C 66.03, H 5.12, N 5.92, found: C 65.83, H 5.23, N 5.83.

*6.1.7. General procedure for preparation of the E and Z 4-(aryl) piperidin-3-one O-4-benzyl oxime ether hydrochlorides **1**–**10**·**HCl***

To a solution of **22**–**26** (0.42 mmol) in EtOH anhydrous (25 mL), was added a solution of EtOH·HCl to pH ≅ 3. The mixture was shaken under hydrogen at room temperature and atmospheric pressure for 30 h in the presence of 10% Pd on charcoal (75 mg), then the catalyst was filtered off and the solution was evaporated to yield a 1:1.5 mixture of *E* and *Z* piperidine hydrochlorides. The pure *E* (**1**,**3**,**5**,**7**,**9**·**HCl**) and *Z* (**2**,**4**,**6**,**8**,**10**·**HCl**) N-unsubstituted piperidine hydrochlorides were obtained by preparative TLC eluting with a mixture of $CH_2Cl_2$:hexane:$NEt_3$ 7.5:1.5:1 (**1**,**2**,**9**,**10**) or $CH_2Cl_2$:hexane:$NEt_3$ 6:3:1 (**3**–**8**).

*6.1.7.1. 4-(4-Fluorophenyl)piperidin-3-one O-4-fluorobenzyl oxime hydrochlorides (**1** E, **2** Z).* **1**·**HCl:** $^1$H NMR (200 MHz, $CDCl_3$) $\delta$ = 7.31–6.96 (m, 8H), 5.07 (s, 2H), 4.78 (m, 1H); 3.52 (d, $J$ = 14.4 Hz, 1H), 3.32 (d, $J$ = 14.4 Hz, 1H), 3.05–2.88 (m, 2H), 2.36–1.99 ppm (m, 2H); Anal. calcd for $C_{18}H_{19}ClF_2N_2O$: C 61.28, H 5.43, N 7.94, found C 61.53, H 5.61, N 8.15. **2**·**HCl**: $^1$H NMR (200 MHz, $CDCl_3$) $\delta$ = 7.27–6.94 (m, 8H), 4.91 (s, 2H), 3.93 (d, $J$ = 15.2 Hz, 1H), 3.63 (m, 1H), 3.49 (d, $J$ = 15.2 Hz, 1H), 3.12–2.83 (m, 2H), 2.13–1.97 ppm (m, 2H); Anal. calcd for $C_{18}H_{19}ClF_2N_2O$: C 61.28, H 5.43, N 7.94, found: C 60.07, H 5.25, N 7.75.

*6.1.7.2. 4-(4-Fluorophenyl)piperidin-3-one O-4-(trifluoromethyl) benzyl oxime hydrochlorides (**3** E, **4** Z).* **3**·**HCl** $^1$H NMR (200 MHz, $CDCl_3$) $\delta$ = 7.61–6.97 (m, 8H), 5.16 (s, 2H), 4.80 (m, 1H), 3.48 (d, $J$ = 14.5 Hz, 1H), 3.32 (d, $J$ = 14.5 Hz, 1H), 3.13–2.85 (m, 2H), 2.38–2.01 ppm (m, 2H); Anal. calcd for $C_{19}H_{19}ClF_4N_2O$: C 56.65, H 4.75, N 6.95, found: C 56.44, H 4.57, N 6.76. **4**·**HCl** $^1$H NMR (200 MHz, $CDCl_3$) $\delta$ = 7.61–6.94 (m, 8H), 5.03 (s, 2H), 3.99 (d, $J$ = 15 Hz, 1H), 3.66 (m, 1H), 3.56 (d, $J$ = 15 Hz, 1H), 3.13–2.87 (m, 2H), 2.16–2.09 ppm (m, 2H); Anal. calcd for $C_{19}H_{19}ClF_4N_2O$: C 56.65, H 4.75, N 6.95, found: C 56.84, H 4.93, N 7.12.

*6.1.7.3. 4-(4-Fluorophenyl)piperidin-3-one O-2-chlorobenzyl oxime hydrochlorides (**5** E, **6** Z).* **5**·**HCl** $^1$H NMR (200 MHz, $CDCl_3$) $\delta$ = 7.27–7.01 (m, 8H), 5.25 (s, 2H), 4.82 (m, 1H), 3.56 (d, 1H, $J$ = 14.5 Hz), 3.35 (d, 1H, $J$ = 14.5 Hz), 3.12–2.89 (m, 2H), 2.40–2.05 ppm (m, 2H); Anal. calcd for $C_{18}H_{19}Cl_2FN_2O$: C 58.55, H 5.19, N 7.59, found: C 58.71, H, 5.36, N 7.72. **6**·**HCl** $^1$H NMR (200 MHz, $CDCl_3$) $\delta$ = 7.27–6.99 (m, 8H), 5.12 (s, 2H), 3.99 (d, 1H, $J$ = 15 Hz), 3.67 (m, 1H), 3.56 (d, 1H, $J$ = 15 Hz), 3.15–2.90 (m, 2H), 2.14–2.09 ppm (m, 2H); Anal. calcd for $C_{18}H_{19}Cl_2FN_2O$: C 58.55, H 5.19, N 7.59, found: C 58.77, H 5.39, N 7.76.

*6.1.7.4. 4-(4-(Trifluoromethyl)phenyl)piperidin-3-one O-4-fluorobenzyl oxime hydrochlorides (**7** E, **8** Z).* **7**·**HCl** $^1$H NMR (200 MHz, $CDCl_3$) $\delta$ = 7.62–6.98 (m, 8H), 5.16 (s, 2H), 4.79 (m, 1H), 3.50 (d, $J$ = 14.5 Hz, 1H), 3.33 (d, $J$ = 14.5 Hz, 1H), 3.15–2.82 (m, 2H), 2.36–1.98 (m, 2H) Anal. calcd for $C_{19}H_{19}ClF_4N_2O$: C 56.65, H 4.75, N 6.95, found: C 56.93, H 4.96, N 7.18. **8**·**HCl** $^1$H NMR (200 MHz, $CDCl_3$) $\delta$ = 7.62–6.96 (m, 8H), 5.04 (s, 2H,), 4.01 (d, $J$ = 15.4 Hz, 1H), 3.66 (m, 1H), 3.58 (d, $J$ = 15.4 Hz, 1H), 3.15–2.88 (m, 2H), 2.17–2.05 ppm (m, 2H). Anal. calcd for $C_{19}H_{19}ClF_4N_2O$: C 56.65, H 4.75, N 6.95, found: C 56.87, H 4.91, N 6.74.

*6.1.7.5. 4-(4-(Trifluoromethyl)phenyl)piperidin-3-one O-2-chlorobenzyl oxime hydrochlorides (**9** E, **10** Z).* **9**·**HCl** $^1$H NMR (200 MHz, $CDCl_3$) $\delta$ = 7.31–6.97 (m, 8H), 5.08 (s, 2H), 4.77 (m, 1H), 3.64 (d, $J$ = 14.5 Hz, 1H), 3.39 (d, $J$ = 14.5 Hz, 1H), 3.19–2.83 (m, 2H), 2.40–2.03 ppm (m, 2H). Anal. calcd for $C_{19}H_{19}Cl_2F_3N_2O$: C 54.43, H 4.57, N 6.68, found: C 54.74, H 4.81, N 6.89. **10**·**HCl** $^1$H NMR (200 MHz, $CDCl_3$) $\delta$ = 7.28–6.96 (m, 8H), 4.94 (s, 2H), 3.99 (d, $J$ = 15.4 Hz, 1H), 3.66 (m, 1H), 3.59 (d, $J$ = 15.4 Hz, 1H), 3.19–2.88 (m, 2H), 2.11–2.04 ppm (m, 2H). Anal. calcd for $C_{19}H_{19}Cl_2F_3N_2O$: C 54.43, H 4.57, N 6.68 found: C 54.71, H 4.39, N 6.87.

### 6.2. Molecular docking

Molecular docking was performed in the homology models of SERT, DAT and NET constructed by Ravna et al. [4], using LeuT as a template [2]. The ligands were built by means of Maestro [35], considering the active enantiomers (3*S*,4*R*)-paroxetine and (*R*)-fluoxetine, and both the enantiomers of compounds **1**–**10**, which were subjected to a Conformational Search (CS) of 1000 steps in a implicit water environment using the Macromodel program [36]. The Monte Carlo algorithm was used with the MMFFs forcefield. The ligands were then minimized using the Conjugated Gradient method to a convergence value of 0.05 kcal/Å mol, using the same forcefield and parameters as for the CS.

The minimized ligands were docked into the proteins using GOLD 3.2 [37]; the region of interest in Gold was defined in such a manner that it contains all the residues which stay within 10 Å from Asp98 of SERT, Asp79 of DAT and Asp75 of NET. The 'allow early termination' command was deactivated, and a 'protein hydrogen bond constraint' set to the value 15 was used to specify that the carboxylic oxygen of Asp98/Asp79/Asp75 of SERT, DAT and NET respectively, should be hydrogen-bonded to the ligand, but without specifying to which ligand atom. The default Gold parameters were used for all remaining variables, and ligands were submitted to 100 Genetic Algorithm runs with the GoldScore fitness function. The best docked pose for each ligand, obtained by clustering the results for 1.5 Å of tolerance, was then used for further studies. Generally at most two or three clusters of solutions were generated, the first was the most populated, and the score difference between the best solution and the second cluster one had a value of about 20. The docking results were visually evaluated using UCSF Chimera [38].

### 6.3. Binding studies

#### 6.3.1. Animals

Cerebral tissue was from adult New Zealand White rabbits (4–5 kg) obtained from a commercial source (Charles River

Laboratories, Inc., Wilmington, MA). Animals were maintained in standard laboratory conditions and feeding in sawdust-lined cages and a 12 h light/dark cycle. They were killed by intravenous injection of a lethal dose of pentobarbital. All procedures conformed to the guidelines of the International European ethical standards for the care and use of laboratory animals. All protocols were approved by the Ethical Deontological Committee for animal experimentation of the University of Pisa.

*6.3.2. Affinity for SERT, NET, DAT*

For SERT binding assays, membranes were prepared from rabbit frontal cortex and [$^3$H]paroxetine (specific activity, 15–20 Ci mmol$^{-1}$; Perkin–Elmer Life Science, Waltham, MA) binding was performed as previously described [39]. The affinity of [$^3$H]-paroxetine for SERT was assessed by saturation experiments obtaining a dissociation constant ($K_d$) value of 56.00 ± 8.00 pM ($n = 3$).

Membranes used in DAT binding assays were prepared from frozen rabbit striatal by homogenization with a polytron homogenizer in a phosphate buffered saline solution (PBS) (25 mM $Na_2HPO_4/NaH_2PO_4$, 48 mM NaCl, pH 7.7 at 4 °C) containing 320 mM sucrose. The homogenate was centrifuged at 46,000*g* for 10 min at 4 °C. The supernatant was discarded and the pellet resuspended by diluting 1:100 (w:v) in the homogenization buffer. The pellet was recentrifuged at 46,000*g* for 10 min and the pellet was resuspended diluted 1:100 in PBS containing sucrose, divided in 1.0 mL aliquots and stored frozen at −80 °C. On the day of the experiment, one or more aliquots were quickly thawed at 37 °C, centrifuged at 46,000*g* for 10 min at 4 °C and the pellet was resuspended in the binding assay buffer at a 1:200 (w:v) dilution.

Cortical membranes for NET binding assays were prepared by homogenizing freshly dissected cerebral cortex in 30 vols of ice-cold 50 mM Tris–HCl buffer, pH 7.4, containing 120 mM NaCl and 5 mM KCl. The homogenate was centrifuged at 46,000*g* for 10 min at 4 °C. The resulting pellet was suspended in 30 vols of 50 mM Tris–HCl buffer, pH 7.4, containing 120 mM NaCl and 5 mM KCl, incubated at 37 °C for 10 min to remove endogenous norepinephrine and centrifuged at 46,000*g* for 10 min at 4 °C. This washing procedure was repeated twice. The resulting pellet was immediately used in the binding assay or frozen at −80 °C until the time of the assay.

Protein concentration was determined according to the method of Lowry et al. [40] using BSA as standard.

For DAT binding assays, striatal membranes (0.2 mg of protein) were incubated in 0.5 mL of a Tris–HCl saline buffer (50 mM Tris–HCl, pH 7.4, 120 mM NaCl, 5 mM KCl) with 0.5–2 nM [$^3$H]-WIN 35,428 (specific activity, 84.5 Ci mmol$^{-1}$; Perkin–Elmer Life Science, Waltham, MA) for 2 h at 4 °C. Non-specific binding was defined in the presence of 10 mM dopamine and was subtracted from total binding to obtain specific binding. Ligand bound to the transporter was separated from free ligand by filtration using a 30-well manifold (Brandel Harvester, Brandel, Gaithersburg, MD) with glass–fiber filters (GF/C) pre-soaked for 2 h at room temperature with 0.6% (w:v) polyethylenimine. Filters were quickly washed three times with ice-cold 50 mM TRIS–HCl, pH 7.4, placed into scintillation vials and soaked overnight in 3 mL of Cytoscint ES (MP Biomedicals Solon, OH). The following day, samples were read by scintillation spectroscopy in a β-counter (Perkin–Elmer Life Science, Waltham, MA). The affinity of [$^3$H]-WIN 35,428 for DAT was assessed by saturation experiments obtaining a $K_d$ value of 6.1 ± 0.3 nM ($n = 3$).

For NET binding assays, [$^3$H]nisoxetine binding was performed essentially as described by Tejani-Butt et al. [41]. The cortical membrane pellet was resuspended in 50 mM Tris–HCl buffer, pH 7.4, containing 300 mM NaCl and 5 mM KCl. The binding assay was performed incubating aliquots of membranes (0.2–0.3 mg of protein) in 50 mM Tris–HCl buffer, pH 7.4, containing 300 mM NaCl and 5 mM KCl with 1 nM [$^3$H]nisoxetine (specific activity, 80 Ci/mmol; Perkin–Elmer Life Science, Waltham, MA) in a final volume of 0.5 mL. Incubation was carried out at 4 °C for 4 h. Non-specific binding was defined in the presence of 10 μM desipramine. Specific binding was obtained by subtracting non-specific binding from total binding and approximated to 85–90% of total binding. The binding reaction was concluded by filtration through Whatman GF/C glass-fiber filters using a Brandel Harvester (see above). Filters were washed four times with 5 mL of the ice-cold binding buffer and placed in vials with 4 mL of a scintillation cocktail. Radioactivity was measured by means of a β-counter (see above). The affinity of [$^3$H]nisoxetine for NET was assessed by saturation experiments and $K_d$ value of 1.5 ± 0.07 nM ($n = 3$) was obtained.

Stock solutions (1 mM) of the test compounds were prepared in ethanol and then diluted in Tris–HCl saline buffer at the required concentration. Competition binding assays were performed with at least seven different concentrations of the test compounds.

*6.3.3. Analysis of data*

Saturation data were analysed and fitted by the non-linear regression analysis of the GraphPad Prism (Version 3.00) computer program (GraphPad Software). The calculated dissociation constant ($K_d$) values for [$^3$H]-paroxetine and [$^3$H]-nisoxetine binding to rabbit cortical membranes were 56.00 ± 8.00 pM ($n = 3$) and 1.50 ± 0.07 nM ($n = 3$), respectively, while the calculated $K_d$ value for [$^3$H]-WIN 35,428, binding to rabbit striatal membranes was 6.10 ± 0.30 nM ($n = 3$). The inhibition curves of the synthesized compounds were analysed and fitted by the non-linear regression analysis of the GraphPad Prism (Version 3.00) computer program (GraphPad Prism, Inc., San Diego, CA). The derived $IC_{50}$ values were used to calculate the inhibition constants ($K_i$) by the Cheng and Prusoff equation [28].

$K_i$ values are presented as the means ± s.e.m. of three independent experiments performed in duplicate.

## Acknowledgements

The authors thank Aina W. Ravna that generously provided the SERT, NET, DAT models.

## Appendix A. Supplementary material

Supplementary material associated with this article can be found, in the online version, at doi:10.1016/j.ejmech.2010.12.018.

## References

[1] S.K. Yamashita, T. Singh, Y. Jin Kawate, E. Gouaux, Nature 437 (2005) 215–223.
[2] W. Ravna, M. Jarończyk, I. Sylte, Bioorg. Med. Chem. Lett. 16 (2006) 5594–5597.
[3] M. Jarończyk, Z. Chilmonczyk, A.P. Mazurek, G. Nowak, A.W. Ravna, K. Kristiansen, I. Sylte, Bioorg. Med. Chem. 16 (2008) 9283–9294.
[4] A.W. Ravna, I. Sylte, S.G. Dahl, J. Mol. Model. 15 (2009) 1155–1164.
[5] S.G. Buttler, M.J. Meegan, Curr. Med. Chem. 15 (2008) 1737–1761.
[6] L. Iversen, Brit. J. Pharmacol. 147 (2006) 582–588.
[7] P.R. Finely, Ann. Pharmacother 28 (1994) 1359–1369.
[8] M.J. Owens, J. Clin. Psychiatry 65 (Suppl. 4) (2004) 5–10.
[9] P. Pacher, V. Kecskemeti, Curr. Med. Chem. 11 (2004) 925–943.
[10] D. Spinks, G. Spinks, Curr. Med. Chem. 9 (2002) 799–810.
[11] L.L. Iversen, R.A. Glennon., Antidepressants. in: D.J. Abraham (Ed.), Burger's Medicinal Chemistry and Drug Discovery, sixth ed., Nervous System Agents, vol. 6 Wiley, New York, 2003, pp. 483–524.
[12] M.D. Dorsey, S.E. Lukas, S.L. Cunningham, Neuropsychopharmacology 14 (1996) 437–442.
[13] S.A. Montgomery, D.S. Baldwin, A. Riley, J. Affect. Disord. 69 (2002) 119–140.
[14] S.H. Kennedy, Eur. Neuropsychopharmacol. 16 (2006) S619–S624.
[15] S.M. Stahl, J. Clin. Psychiatry 59 (1998) 343–344.

[16] M.J. Owens, W.N. Morgan, S.J. Plott, C.B. Nemeroff, J. Pharmacol. Exp. Therap. 283 (1997) 1305–1322.
[17] M.J. Owens, D.L. Knight, C.B. Nemeroff, Biol. Psychiatry 47 (2000) 842–845.
[18] M.J. Owens, D.L. Knight, C.B. Nemeroff, Biol. Psychiatry 50 (2001) 345–350.
[19] R.W. Lam, Int. J. Psych. Clin. Practice 8 (Suppl. 1) (2004) 25–29.
[20] F. Chen, M.B. Larsen, C. Sànchez, O. Wiborg, Eur. Neuropsychopharmacol. 15 (2005) 193–198.
[21] S. Schreiber, C.G. Pick, Eur. Neuropsychopharmacol. 16 (2006) 464–468.
[22] S.M. Stahl, Int. J. Psych. Clin. Practice 8 (Suppl. 1) (2004) 3–10.
[23] S. Källströ, R. Leino, Bioorg. Med. Chem. 16 (2008) 601–605.
[24] A. Balsamo, A. Lapucci, M. Macchia, B. Macchia, A. Martinelli, S. Nencetti, A. Rossello, T. Cristina, Il Farmaco 49 (1994) 77–82.
[25] A. Balsamo, A. Lapucci, A. Lucacchini, M. Macchia, C. Martini, C. Nardini, S. Nencetti, Eur. J. Med. Chem. 29 (1994) 967–973.
[26] Our unpublished results.
[27] G.J. Karabatsos, N. Hsi, Tetrahedron 23 (1967) 1079–1095.
[28] Y. Cheng, W.H. Prusoff, Biochem. Pharmacol. 22 (1973) 3099–3108.
[29] A. Lipinski, F. Lombardo, B.W. Dominy, P.J. Feeney, Adv. Drug Deliv. Rev. 23 (1997) 3–25.
[30] S. Tavoulari, L.R. Forrest, G. Rudnick, J. Neurosci. 29 (2009) 9635–9643.
[31] L. Celik, S. Sinning, K. Severinsen, C.G. Hansen, M.S. Møller, M. Bols, O. Wiborg, B. Schiøtt, J. Am. Chem. Soc. 130 (2008) 3853–3865.
[32] S.M. Cloonan, J.J. Kating, S.G. Butler, A.J. Knox, A.M. Jørgensen, G.H. Peters, D. Rai, D. Corrigan, D.G. Lloyd, D.C. Williams, M.J. Meegan., Eur. J. Med. Chem. 44 (2009) 4862–4888.
[33] B. Wenzel, D. Sorger, K. Heinitz, M. Scheunemann, R. Schliebs, J. Steinbach, O. Sabri, Eur. J. Med. Chem. 40 (2005) 1197–1205.
[34] C. Morrill, N.S. Mani, Org. Lett. 9 (2007) 1505–1508.
[35] Maestro, ver. 7.5. Schrödinger Inc., Portland, OR, 1999.
[36] Macromodel, ver. 8.5. Schrödinger Inc., Portland, OR, 1999.
[37] G. Jones, P. Willett, R.C. Glen, A.R. Leach, R.J. Taylor, J. Mol. Biol. 267 (1997) 727–748.
[38] C. Huang, G.S. Couch, E.F. Pettersen, T.E. Ferrin, Pac. Symp. Biocomput. 1 (1996) 724.http://www.cgl.ucsf.edu/chimera.
[39] S. Nencetti, G.C. Demontis, M.R. Mazzoni, L. Betti, I. Banti, A. Rossello, A. Lapucci, J. Pharm. Pharmacol. 59 (2007) 1439–1445.
[40] O.H. Lowry., N.J. Rosenbrough, A.L. Farr, R.J. Randall, J. Biol. Chem. 193 (1951) 265–267.
[41] S.M. Tejani-Butt, D.J. Brunswick, A. Frazer, Eur. J. Pharm. 191 (1990) 239–243.